

The Heptakis-(2,6-di-*O*-methyl)- β -cyclodextrin Inclusion Complex with Acetic Acid

M. SELKTI^{1,*}, A. NAVAZA, F. VILLAIN, P. CHARPIN and C. DE RANGO^{**}
ER5128-CNRS, Centre Pharmaceutique, Université Paris-Sud, 92296 Châtenay-Malabry, France.

(Received: 21 February 1996; in final form: 24 May 1996)

Abstract. A novel monomer-type structure of heptakis-(2,6-di-*O*-methyl)- β -cyclodextrin in a typical monoclinic herringbone scheme has been determined by single crystal X-ray diffraction. Crystal data: space group $P2_1$, $Z = 2$, $a = 15.165(6)$, $b = 10.613(3)$, $c = 23.188(8)$ Å, $\beta = 102.02(4)^\circ$, $V = 3650(3)$ Å³ and $R = 0.094$ for 2933 observed $\text{MoK}\alpha$ reflections with $I > 3\sigma(I)$. A unique water molecule located in the intermolecular spaces, reinforces the cohesion between the herringbone chains. The analysis of the electron density distribution suggests that an acetic acid molecule is trapped within the macrocycle cavity, alternately with a water molecule.

Key words: Methylated β -cyclodextrin, X-ray crystallography, inclusion.

1. Introduction

Methylated β -cyclodextrins are attractive for the formation of inclusion compounds owing to their good solubilities in organic solvents as well as in water [1]; however, among the few crystal structures of heptakis-(2,6-di-*O*-methyl)- β -cyclodextrin (DIMEB) complexes previously reported, only one inclusion compound and one catenane derivative have been described [2, 3]. In the inclusion compound, the guest molecule, adamantanol, disordered over two sites, is fully included within the cavity of the DIMEB molecule. The 1 : 1 crystalline DIMEB complexes formed with carmofur and with disubstituted benzenes such as *p*-iodophenol and *p*-nitrophenol, are not inclusion compounds; indeed, the carmofur is disordered and positioned with its fluorouracil moiety at the exterior of the molecular cavity and with its hexyl group either outside or extended into the host macrocycle [4], while the disubstituted benzenes are excluded from the cavity and situated in intermolecular spaces [5]. In these structures, DIMEB molecules are arranged as monomeric units in layer-type [4] or, as for anhydrous DIMEB, in zigzag chain-type packings [5, 6]. The present structure, in which an acetic acid molecule is detected within the molecular cavity, is the first example of a typical monoclinic herringbone cage-type packing of DIMEB molecules. This crystal feature packing is very similar to that

^{* 1} Present Address: Laboratoire de Physique, Faculté des Sciences Pharmaceutiques et Biologiques de ParisV, 4, avenue de l'Observatoire, 75270 Paris, France.

^{**} Author for correspondence.

of native β -CD hydrates [7] and isomorphous structures (small guest inclusion compounds [8] or monovalent cation (K^+) complex [9]).

2. Experimental

Crystals were grown by slow evaporation of an aqueous solution of DIMEB containing $[UO_2(CH_3COO)_3Na]$ salt in an attempt to obtain a heavy atom DIMEB complex. A colourless crystal of approximate dimensions $0.9 \times 0.4 \times 0.5$ mm was selected, sealed in the presence of the mother liquor in a thin glass capillary and mounted on an Enraf-Nonius CAD-4 diffractometer. Cell constants were determined from setting angles of 25 reflections in the range $7^\circ < \theta < 13^\circ$. Absorption effects were first corrected by the ψ scan procedure [10] and then by refinement from ΔF [11]. Crystallographic data, data collection and structure refinement parameters are summarized in Table I.

The structure was solved straightforwardly by rotation and translation functions using an early version of the *AMoRe* program package [12], with a model structure of native β -CD minus the primary hydroxy groups. The positions of methyl C atoms were determined from successive difference syntheses which did not show any uranyl ion but revealed one fully occupied water site in the intermolecular spaces. Due to the large number of parameters to be refined with respect to the number of observed structure factors, only O atoms were given anisotropic temperature factors except the O(6) atoms of the G5 and G7 residues for which those factors were not satisfactory. For O(67), no disorder was detected from electron density maps while a spurious peak appeared close to O(65) with a separation distance shorter than the crystallographic resolution, indicating a slight unresolvable disorder for this site position. Both atoms were refined with isotropic temperature factors in the correct range. H atoms bonded to C atoms (except those of methyl groups) were introduced in geometrically calculated positions but not refined. Geometrical restraints were applied to handle the refinement convergence. In the last stages of the refinement, residual electron density peaks were localized within the cavity. A detailed analysis of the difference synthesis maps succeeded in positioning one acetic acid molecule with partial occupancy (0.5). The residual peaks in the final $\Delta\rho$ map were smaller than $0.55 \text{ e}\text{\AA}^{-3}$ except two, one ($0.81 \text{ e}\text{\AA}^{-3}$) close to the C(65) atom and a second ($0.70 \text{ e}\text{\AA}^{-3}$) within the cavity. Final atomic coordinates and thermal parameters of the non-H atoms are given in Table II. Refinement was carried out with the SHELX76 program [13] and computer graphics of the electron density maps using the FRODO program [14]. Molecular graphics were performed by the SYBYL program package [15].

3. Discussion

The crystal structure consists of an arrangement of DIMEB monomers which are stacked along the b -axis forming a new herringbone-type pattern (Figure 1). The

Table I. X-ray diffraction experimental details.

Formula	$(C_{56}H_{98}O_{35}) \cdot 1.5(H_2O) \cdot 0.5(CH_3COOH)$
Chemical formula weight	1387
Cell setting	Monoclinic
Space group	$P2_1$
a (Å)	15.165 (6)
b (Å)	10.613 (3)
c (Å)	23.188 (8)
β (°)	102.02 (4)
V (Å ³)	3650 (3)
Z	2
δ_{cal} (g cm ⁻³)	1.22
Radiation type	MoK α
Wavelength (Å)	0.71073
No. of reflections for cell parameters	25
θ range (°)	7–13
μ_{cal} (mm ⁻¹)	0.82
Temperature (K)	295°
<i>Data collection</i>	
Diffractometer	Enraf-Nonius CAD-4
Data collection method	$\omega/2\theta$ scan
θ_{max} (°)	20°
No. of standard reflections	3
Maximum decay (%)	2
Absorption correction	Based on ψ scans, empirical
T_{min}	0.785
T_{max}	0.999
No. of measured reflections	4949
No. of independent reflections	3455
No. of observed reflections	2933
Criterion for observed reflections	$I > 3\sigma(I)$
<i>Refinement</i>	
Refinement on	F
Minimization based on	Sum of $w\Delta F^2$
Final R [$I > 3\sigma(I)$]	0.094
R_w	0.102
S	1.2
No. of parameters used	550
H-atom treatment	Theoretical – not refined
Weighting scheme	$w = 1.854/[\sigma^2(F) + 0.00547F^2]$
$(\Delta/\sigma)_{max}$	0.4
$\Delta\rho_{max}$ (e Å ⁻³)	0.81
$\Delta\rho_{min}$ (e Å ⁻³)	-0.37

Table II. Fractional atomic coordinates and isotropic or equivalent isotropic displacement parameters (\AA^2) for non-H atoms.

	<i>x</i>	<i>y</i>	<i>z</i>	$U_{\text{eq}}/U_{\text{iso}}$
O(41)	-0.2817 (5)	0.0000	0.1423 (3)	0.043 (5)*
C(11)	-0.2284 (8)	-0.2732 (13)	0.0282 (6)	0.053 (4)
C(21)	-0.2845 (9)	-0.1627 (11)	0.0017 (5)	0.045 (4)
C(31)	-0.2737 (9)	-0.0562 (11)	0.0442 (5)	0.040 (3)
C(41)	-0.3013 (9)	-0.0994 (11)	0.1005 (5)	0.044 (4)
C(51)	-0.2503 (9)	-0.2201 (11)	0.1246 (5)	0.043 (4)
C(61)	-0.2841 (9)	-0.2762 (14)	0.1768 (6)	0.057 (4)
O(21)	-0.2560 (7)	-0.1233 (10)	-0.0502 (4)	0.068 (7)*
O(31)	-0.3289 (7)	0.0466 (9)	0.0205 (4)	0.060 (7)*
O(51)	-0.2596 (6)	-0.3134 (8)	0.0798 (4)	0.052 (6)*
O(61)	-0.3765 (6)	-0.2995 (10)	0.1593 (5)	0.064 (7)*
O(42)	-0.1838 (5)	0.2131 (8)	0.3117 (3)	0.040 (5)*
C(12)	-0.3523 (8)	0.0460 (11)	0.1675 (5)	0.040 (3)*
C(22)	-0.3480 (8)	0.1892 (11)	0.1699 (5)	0.043 (3)
C(32)	-0.2661 (8)	0.2342 (11)	0.2138 (5)	0.041 (3)
C(42)	-0.2632 (8)	0.1725 (11)	0.2726 (5)	0.043 (4)
C(52)	-0.2659 (8)	0.0299 (11)	0.2645 (5)	0.040 (3)
C(62)	-0.2646 (10)	-0.0390 (14)	0.3209 (6)	0.055 (4)
O(22)	-0.3453 (6)	0.2253 (8)	0.1108 (4)	0.057 (6)*
O(32)	-0.2719 (7)	0.3678 (8)	0.2189 (5)	0.063 (7)*
O(52)	-0.3476 (5)	-0.0037 (8)	0.2250 (3)	0.044 (5)*
O(62)	-0.3343 (8)	0.0035 (13)	0.3480 (4)	0.085 (8)*
O(43)	0.0876 (5)	0.2740 (8)	0.4111 (3)	0.041 (5)*
C(13)	-0.1862 (9)	0.2483 (12)	0.3700 (5)	0.050 (4)
C(23)	-0.1483 (9)	0.3806 (13)	0.3810 (7)	0.057 (7)
C(33)	-0.0496 (8)	0.3785 (12)	0.3789 (6)	0.048 (4)
C(43)	-0.0007 (7)	0.2816 (11)	0.4219 (6)	0.040 (3)
C(53)	-0.0452 (8)	0.1529 (11)	0.4087 (6)	0.042 (3)
C(63)	-0.0058 (10)	0.0569 (12)	0.4543 (6)	0.059 (4)
O(23)	-0.1998 (7)	0.4595 (9)	0.3385 (5)	0.073 (7)*
O(33)	-0.0136 (7)	0.4990 (9)	0.3945 (5)	0.066 (7)*
O(53)	-0.1390 (5)	0.1626 (9)	0.4103 (4)	0.049 (6)*
O(63)	-0.0421 (7)	-0.0663 (10)	0.4414 (5)	0.075 (8)*
O(44)	0.3388 (5)	0.1677 (9)	0.3615 (3)	0.047 (6)*
C(14)	0.1599 (8)	0.2930 (12)	0.4591 (6)	0.047 (4)
C(24)	0.2240 (9)	0.3905 (12)	0.4443 (6)	0.052 (4)
C(34)	0.2702 (9)	0.3417 (11)	0.3968 (6)	0.048 (4)
C(44)	0.3109 (9)	0.2160 (11)	0.4121 (6)	0.047 (4)
C(54)	0.2437 (9)	0.1258 (12)	0.4304 (6)	0.052 (4)
C(64)	0.2837 (9)	-0.0007 (12)	0.4540 (6)	0.066 (5)
O(24)	0.1725 (7)	0.5003 (9)	0.4251 (5)	0.067 (7)*
O(34)	0.3363 (7)	0.4300 (9)	0.3898 (5)	0.075 (8)*
O(54)	0.2066 (6)	0.1809 (9)	0.4768 (4)	0.050 (6)*
O(64)	0.3581 (8)	0.0199 (11)	0.5023 (5)	0.087 (8)*

Table II. Continued.

	x	y	z	$U_{\text{eq}}/U_{\text{iso}}$
O(45)	0.3675 (5)	-0.0494 (8)	0.2097 (3)	0.045 (5)*
C(15)	0.4301 (9)	0.1427 (13)	0.3643 (6)	0.060 (4)
C(25)	0.4622 (10)	0.1999 (13)	0.3133 (6)	0.062 (4)
C(35)	0.4115 (9)	0.1397 (11)	0.2569 (5)	0.047 (4)
C(45)	0.4248 (9)	-0.0021 (11)	0.2601 (5)	0.048 (4)
C(55)	0.3988 (10)	-0.0512 (12)	0.3153 (6)	0.055 (4)
C(65)	0.4261 (14)	-0.1924 (13)	0.3246 (8)	0.104 (7)
O(25)	0.4452 (7)	0.3326 (10)	0.3151 (5)	0.080 (8)*
O(35)	0.4451 (7)	0.1861 (9)	0.2077 (4)	0.063 (7)*
O(55)	0.4476 (7)	0.0131 (10)	0.3666 (5)	0.075 (8)*
O(65)	0.4136 (13)	-0.2285 (15)	0.3790 (7)	0.152 (6)
O(46)	0.1559 (6)	-0.2533 (8)	0.0764 (4)	0.051 (6)*
C(16)	0.4049 (10)	-0.1375 (12)	0.1747 (6)	0.056 (4)
C(26)	0.3801 (9)	-0.1007 (13)	0.1105 (6)	0.054 (4)
C(36)	0.2812 (8)	-0.1153 (12)	0.0850 (5)	0.047 (4)
C(46)	0.2507 (8)	-0.2478 (12)	0.0985 (5)	0.050 (4)
C(56)	0.2763 (10)	-0.2705 (13)	0.1640 (6)	0.056 (4)
C(66)	0.2527 (14)	-0.4032 (16)	0.1810 (8)	0.097 (6)
O(26)	0.4094 (6)	0.0234 (9)	0.1069 (4)	0.059 (7)*
O(36)	0.2619 (7)	-0.0903 (11)	0.0236 (4)	0.075 (8)*
O(56)	0.3724 (7)	-0.2594 (8)	0.1828 (4)	0.065 (7)*
O(66)	0.2584 (15)	-0.4059 (17)	0.2432 (6)	0.157 (16)*
O(47)	-0.1376 (5)	-0.2367 (8)	0.0432 (5)	0.056 (6)*
C(17)	0.1208 (9)	-0.3623 (14)	0.0455 (6)	0.058 (4)
C(27)	0.0661 (9)	-0.3221 (15)	-0.0131 (6)	0.066 (4)
C(37)	-0.0163 (9)	-0.2511 (14)	-0.0068 (6)	0.062 (4)
C(47)	-0.0694 (8)	-0.3216 (13)	0.0310 (5)	0.048 (4)
C(57)	-0.0059 (10)	-0.3573 (16)	0.0887 (6)	0.070 (5)
C(67)	-0.0542 (12)	-0.4397 (19)	0.1270 (8)	0.090 (6)
O(27)	0.1229 (8)	-0.2469 (13)	-0.0403 (5)	0.092 (9)*
O(37)	-0.0717 (7)	-0.2318 (12)	-0.0641 (4)	0.081 (8)*
O(57)	0.0670 (6)	-0.4288 (8)	0.0776 (5)	0.063 (7)*
O(67)	-0.0015 (13)	-0.432 (2)	0.1856 (9)	0.163 (7)
C(71)	-0.4124 (12)	-0.3548 (18)	0.2060 (8)	0.081 (5)
C(72)	-0.3262 (14)	-0.047 (2)	0.4046 (8)	0.100 (6)
C(73)	0.0005 (15)	-0.134 (2)	0.4007 (9)	0.099 (7)
C(74)	0.3959 (17)	-0.097 (2)	0.5228 (11)	0.131 (9)
C(75)	0.4806 (19)	-0.324 (3)	0.4023 (12)	0.158 (10)
C(76A)	0.203 (4)	-0.500 (5)	0.262 (2)	0.21 (2)
C(76B)	0.179 (5)	-0.390 (16)	0.265 (4)	0.21 (2)
C(77)	-0.046 (2)	-0.484 (3)	0.2286 (12)	0.166 (11)
C(81)	-0.2969 (13)	-0.187 (2)	-0.1019 (8)	0.094 (6)
C(82)	-0.3815 (13)	0.3482 (16)	0.0965 (8)	0.087 (6)
C(83)	-0.2159 (17)	0.582 (2)	0.3577 (11)	0.121 (8)
C(84)	0.2160 (14)	0.6180 (17)	0.4430 (9)	0.094 (6)
C(85)	0.4997 (16)	0.409 (2)	0.2882 (10)	0.117 (7)
C(86)	0.4375 (10)	0.0520 (15)	0.0521 (6)	0.060 (4)
C(87)	0.1189 (13)	-0.275 (2)	-0.1006 (8)	0.097 (6)

Table II. Continued.

	x	y	z	$U_{\text{eq}}/U_{\text{iso}}$
OW(1)	-0.5048 (13)	-0.316 (2)	0.0487 (9)	0.165 (7)
OW(2)	-0.039 (4)	-0.058 (6)	0.241 (2)	0.205 (19)
CG(1)	0.070 (2)	0.088 (4)	0.2258 (16)	0.217 (13)
CG(2)	0.121 (2)	0.208 (4)	0.2333 (16)	0.217 (13)
OG(1)	0.011 (2)	0.057 (4)	0.2497 (16)	0.217 (13)
OG(2)	0.097 (2)	0.010 (4)	0.1885 (16)	0.217 (13)

$U_{\text{eq}} = (1/3) \sum_i \sum_j U_{ij} a_i^* a_j^* \mathbf{a}_i \cdot \mathbf{a}_j$ for starred atoms, U_{iso} for others.

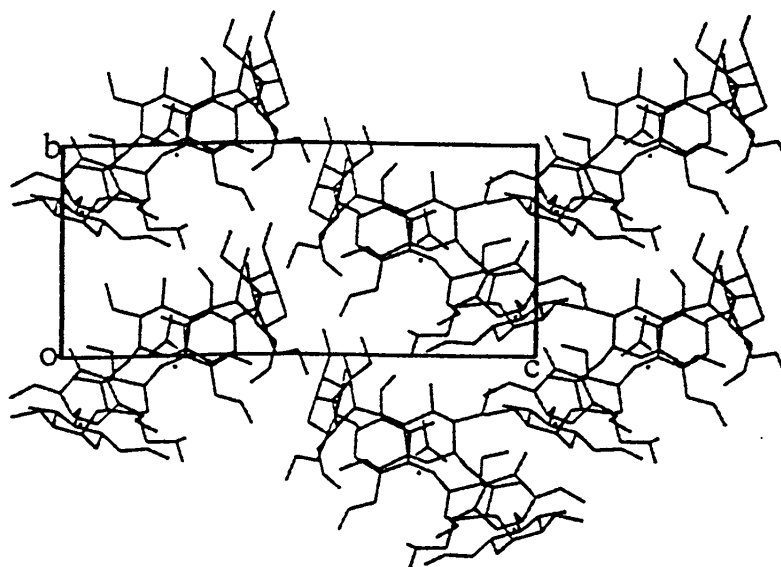


Figure 1. Packing view of the structure down the a -axis. The herringbone (HB) chains of DIMEB monomers run parallel to the vertical b -axis.

structure containing a unique interstitial water molecule per DIMEB molecule, is stabilized by intermolecular $\text{C} \cdots \text{O}$ contacts involving C methyl and O atoms of the macrocycle.

3.1. MACROCYCLE CONFORMATION

Except for the orientation of the methyl groups, the macrocycle conformation does not significantly differ from that of unmodified β -CD as observed in the previously reported structures of DIMEB complexes. The average bond distances and angles are in the usual range for the glucopyranose residues. The DIMEB molecular unit is presented in Figure 2. Geometrical data describing the conformation of the

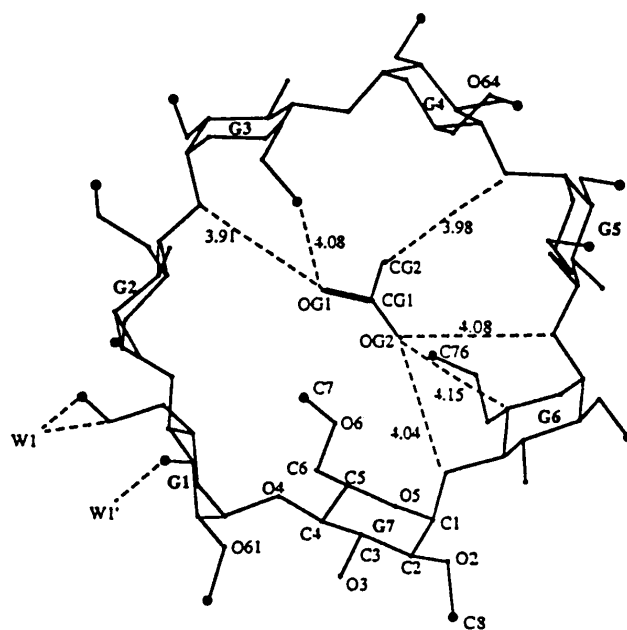


Figure 2. The DIMEB molecular unit with the closest van der Waals contact distances between the acetic acid molecule and the macrocycle. For clarity, only the major site of C(76) is represented. Atom labeling is indicated, C(*mn*) or O(*mn*) denotes atoms with the *n*th glucopyranose residue (G*n*).

Table III. Geometrical data describing the conformation of the DIMEB macrocycle.

Residue	O(4) distance from O(4) plane (Å)	O(2) distance from O(2)/O(3) plane (Å)	O(3) distance from O(2)/O(3) plane (Å)	O(6) distance from O(6) plane (Å)	Tilt* (°)
G1	0.26	-0.11	0.25	0.20	16 (2)
G2	0.03	0.53	0.43	0.31	4 (2)
G3	-0.23	-0.27	-0.33	-0.73	20 (1)
G4	0.03	-0.37	-0.18	0.33	16 (2)
G5	0.25	0.21	0.41	0.08	5 (2)
G6	-0.16	0.31	0.18	-0.01	10 (2)
G7	-0.17	-0.57	-0.49	-0.19	27 (1)

* Tilt angles are defined as the dihedral angles between the O(4) plane and the O(4) (*n* - 1), C(1)*n*, C(4)*n*, O(4)*n* least-squares planes.

macrocycle are summarized in Table III and a selection of torsion angles is given in Table IV.

The maximal deviation of the O(4) atoms to their least-squares plane is less than 0.26 Å. The distances O(4)*n*—O(4)(*n* + 1) range from 4.28 to 4.52 Å and the heptagon radii (distance from the center of gravity) from 4.92 to 5.26 Å. All residues

Table IV. Selected torsion angles.

Residue	Torsion ($^{\circ}$)	Torsion ($^{\circ}$)	Torsion ($^{\circ}$)
	O(5)—C(5)—C(6)—O(6)	C(5)—C(6)—O(6)—C(7)	C(1)—C(2)—O(2)—C(8)
G1	-65 (2)	179 (2)	86 (2)
G2	-66 (2)	-172 (2)	153 (2)
G3	64 (2)	83 (3)	143 (2)
G4	-66 (2)	-178 (2)	143 (2)
G5	52 (2)	-148 (2)	156 (2)
G6	75 (3)	154 (3)	148 (2)
G7	79 (3)	169 (3)	135 (2)

incline with their O(6) side towards the inside of the macrocycle, two (G3 and G7) exhibiting a tilt angle higher than 20° , as observed in structures of *p*-iodophenol and *p*-nitrophenol DIMEB complexes. Three C(6)—O(6) bonds are directed outwards (*gg* conformation) from the cavity and the other four (*gt* conformation) towards the molecular axis, above the cavity. One of the O(6) atoms in *gg* conformation, O(61), is at hydrogen bonding distance from the water molecule, a second, O(64), at close contact distance from one 6-*O*-methyl group of an adjacent molecule. One 6-*O*-methyl group, C(76), is disordered over two sites with respective occupancies of 0.7 and 0.3. The torsion angles involving the 6-*O*-methyl groups show a *trans* conformation of the O(6)—C(7) bond relative to the C(5)—C(6) bond for all residues except G3 and the minor site of G6. Each 2-*O*-methyl group points away from the macrocycle, the O(2)—C(8) bond is approximately *gauche* with respect to the C(1)—C(2) bond with a torsion angle of 86° for G1, while the torsion angle of the six other residues has a mean value of 146° .

The intramolecular hydrogen bonds between the O(3)H hydroxy groups and the O(2)CH₃ methoxy groups of adjacent residues maintain the round shape of the macrocycle, the related O(2)*n* ··· O(3)(*n* - 1) distances ranging from 2.76 to 3.10 Å.

3.2. CRYSTAL PACKING

The DIMEB molecules are inclined, as monomeric units, at 56° along the twofold screw axis, giving rise to infinite chains in a classical herringbone (HB) scheme. The HB chains form sheets parallel to the *ab* plane which are stacked along the *c*-axis (Figure 3). Such an arrangement has not yet been observed for DIMEB, although previously reported for hexakis-(2,6-di-*O*-methyl)- α -cyclodextrin inclusion compounds with iodine and 1-propanol [16].

The cohesion of the structure is ensured by intermolecular C ··· O contacts involving 6-*O*- or 2-*O*-methyl groups and O atoms of the macrocycle. A selection of such contacts with related distances less than 3.6 Å is given in Table V. It is likely that some of them might be due to C—H ··· O hydrogen bonds similar to those

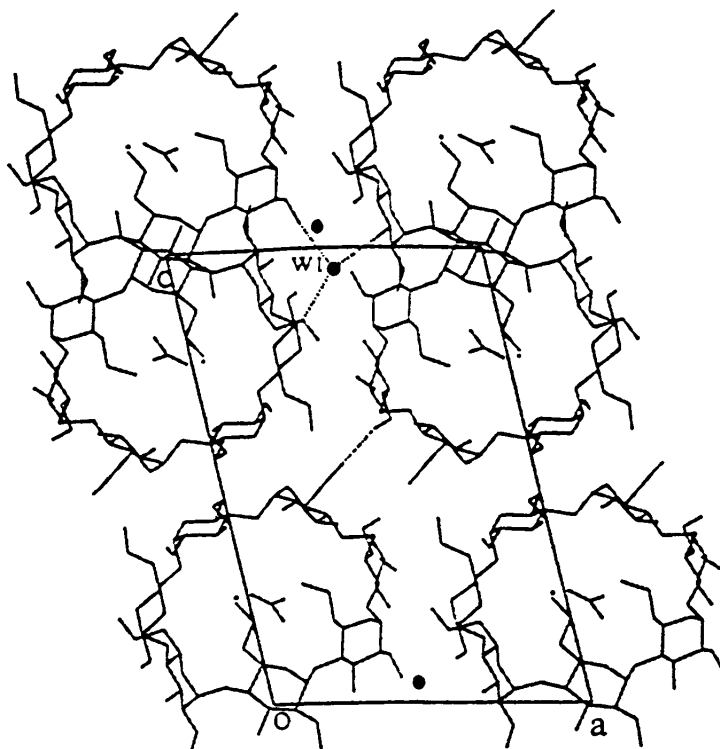


Figure 3. View of the structure along the b -axis, illustrating the role of W1 (full circle, interactions in dashed lines) between HB chains in the sheets and indicating the C(75) \cdots O(64) close contact (dashed line) between monomers of adjacent sheets.

described for carbohydrate structures from analysis of neutron diffraction data [17] and for the anhydrous DIMEB structure [6]. These contacts are frequent between monomers located within the same HB chain, but they involve uniquely secondary hydroxyls, while only two contacts are observed between monomers from adjacent HB chains inside a sheet, both formed with O(5) atoms. The packing of sheets is stabilized by only one C \cdots O contact which links through the 6- O -methyl group of G5 and the O(6) atom of G4, two monomers of adjacent sheets (Figure 3). The unique interstitial O(W1) water molecule, hydrogen bonded simultaneously to two DIMEB molecules from HB chains of the same sheet (O(W1) \cdots O(61), 2.89 Å; O(W1) \cdots O(31)^{*i*}, 3.06 Å, symmetry code: (*i*) = 1 - x , y - 1/2, - z), reinforces the cohesion inside the sheets. Moreover, O(W1) being at a short distance (3.07 Å) from one 2- O -methyl group, C(86), affected by a low thermal motion, might be involved in a C—H \cdots O interaction (C(86)^{*j*} \cdots O(W1), symmetry code: (*j*) = x , y - 1/2, - z) contributing jointly with the hydrogen bond O(W1) \cdots O(61) to form a bridge between monomers of the same HB chain.

The role played by O(W1) in the cohesion of the structure is to compare with that of the characteristic water molecule always present in all hydrate and

Table V. Intermolecular C···O close contacts (<3.6 Å).

C(81)—O(35) ^a	3.26 (3)
C(81)—O(26) ^a	3.51 (3)
C(87)—O(22) ^a	3.49 (3)
C(75)—O(34) ^b	3.38 (4)
C(76A)—O(34) ^b	3.31 (4)
C(71)—O(56) ^c	3.35 (3)
C(72)—O(55) ^c	3.42 (3)
C(75)—O(64) ^d	3.37 (3)

Symmetry codes: (a) $-x, y - 1/2, -z$; (b) $x, y - 1, z$; (c) $x - 1, y, z$; (d) $1 - x, y - 1/2, -z + 1$.

isomorphous HB-type structures of native β -CD. This water molecule is observed as hydrogen bonded to hydroxy groups but never to other water molecules and it is even replaced by the cation K^+ in the KOH/ β -CD complex [9]. In these HB-type structures, the overall packing is always stabilized by intermolecular hydrogen bonds between hydroxy groups ensuring the cohesion of the structure within the HB chains and inside the sheets; however, there are no short contacts between monomers of different sheets. The cohesion between the sheets is essentially due to hydrogen bonds involving two pairs of water molecules which frequently exhibit statistic disorder and slight different positions depending on the water content per β -CD molecule [18].

In the present DIMEB complex the monomers are more tilted with respect to the b -axis than unmodified β -CD molecules in HB-type structures (inclination of the O(4) plane, 56° instead of 45°), the crystal lattice contains only the ‘permanent’ water molecule and the stability of the structure is predominantly ensured by C···O contacts. Nevertheless, the stacking modes of monomers within HB chains as well as HB chains inside sheets are similar in both classes of structures with similar a and b parameters of the unit cells. As expected, differences occur in the packing of adjacent sheets along the c -axis mainly due to the more sterically demanding local environment of methoxy groups around the DIMEB molecules. These differences may be also related to the absence of interstitial water pairs essential to the cohesion of the packing of sheets in native β -CD structures; in the present structure the sheets are held together by a unique C···O contact involving the 6-*O*-methyl group of G5.

3.3. THE GUEST MOLECULES

In the last step of the refinement, several residual electron density peaks (about $1 \text{ e } \text{Å}^{-3}$) situated within the cavity could not be directly interpreted. An analysis

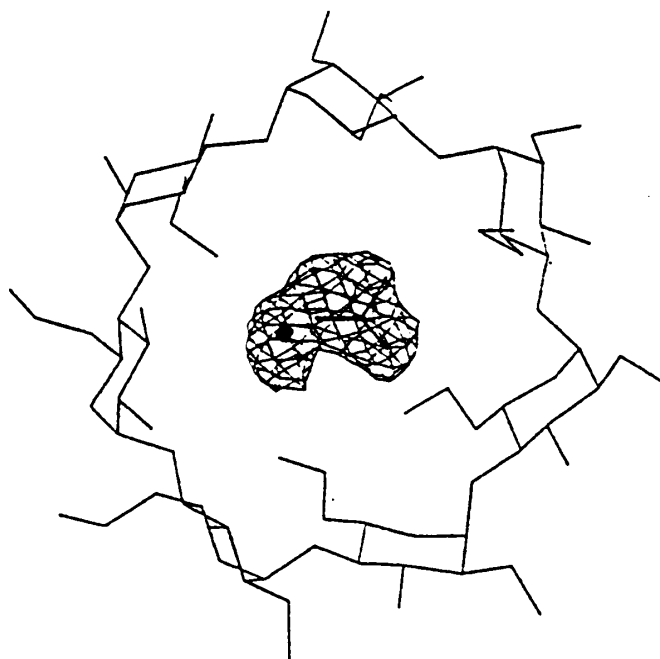


Figure 4. Residual electron density with no guest molecule contribution contoured at $0.5 \text{ e } \text{\AA}^{-3}$, viewed along the molecular axis.

of the electron density maps displayed by computer graphic programs led us to suggest that this area may be alternately occupied by either one acetic acid or one water molecule.

The difference Fourier map calculated without any guest molecule contribution, represented in Figure 4, revealed one flattened electron density area. The prominent part of this irregularly shaped area has been interpreted as a water molecule. A further difference synthesis calculated with contribution of this water molecule (occupancy 0.5), showed that one acetic acid molecule could fit the residual electron density. The peaks initially observed in the difference Fourier map were eliminated when introducing these molecules, both with an occupancy factor of 0.5 estimated approximately from the height of the electron density. In the final stage of the refinement, the coordinates of the acetic acid molecule were optimized by the block rigid group procedure. The stereochemical parameters of the acetic acid molecule were provided from a previously reported structure [19]. No residual electron density peaks higher than $0.55 \text{ e } \text{\AA}^{-3}$ were detected within the cavity in the last difference synthesis, except one near the acetic acid molecule ($0.70 \text{ e } \text{\AA}^{-3}$).

The short separation between the water molecule, O(W2), and one O atom of the acetic acid (O(W2) \cdots O(G1), 1.43 \AA) implies that only one out of the two guest molecules is present within a cavity. The acetic acid molecule is positioned approx-

imately at the center of the macrocycle and straddles the O(4) plane, inclined at about 50° . No short contacts occur between the guest molecules and the macrocycle atoms as shown in Figure 2 which indicates the closest van der Waals contacts for the acetic acid molecule. It is likely that these detected guest molecules have little effect on the packing characteristics of the DIMEB molecules.

4. Concluding Remarks

This study illustrates the predominant role of intermolecular C—H \cdots O interactions involving the methoxy groups when methylation of the O(6)H and O(2)H hydroxy groups blocks the formation of (O—H \cdots O) hydrogen bond networks through β -CD hydroxy groups and water molecules. Moreover, it is pointed out that the unique interstitial water molecule in the present structure can be compared to the 'permanent' water molecule never hydrogen bonded to other water molecules in monoclinic HB-type structures of native β -CD.

A further piece of information from the crystal structure of this DIMEB-sesquihydrate–0.5 acetic acid complex, is the existence of an unexpected guest molecule. In the aqueous solution containing acetate ions and cations from the originally used $[\text{UO}_2(\text{CH}_3\text{COO})_3\text{Na}]$ salt, some acetic acid is presumably present; being more lipophilic than the ions, it is not surprising that it is selectively complexed.

References

1. K. Harata: in J.L. Atwood, J.E.D. Davies, and D.D. MacNicol (eds.), *Inclusion Compounds*, Vol. 5, Oxford University Press (1991), pp. 312–344.
2. M. Czugler, E. Eckle, and J.J. Stezowski: *J. Chem. Soc., Chem. Commun.* 1291 (1981).
3. D. Armspach, P.R. Ashton, C.P. Moore, N. Spencer, J. F. Stoddart, T.J. Wear, and D.J. Williams: *Angew. Chem. Int. Ed. Engl.* **32**, 854 (1993).
4. K. Harata, F. Hirayama, K. Uekama, and G. Tsoucaris: *Chem. Lett.* 1585 (1988).
5. K. Harata: *Bull. Chem. Soc. Jpn.* **61**, 1939 (1988).
6. Th. Steiner and W. Saenger: *Carbohydr. Res.* **275**, 73 (1995).
7. V. Zabel, W. Saenger, and S.A. Mason: *J. Am. Chem. Soc.* **108**, 3664 (1986).
8. W. Saenger: in J.L. Atwood, J.E.D. Davies, and T. Osa (eds.), *Clathrate Compounds, Molecular Inclusion Phenomena, and Cyclodextrins*, D. Reidel Publishing Company, Dordrecht/Boston/Lancaster (1984).
9. P. Charpin, I. Nicolis, C. de Rango, and A.W. Coleman: *Acta Crystallogr.* **C47**, 1829 (1991).
10. A.C.T. North, D.C. Philips, and F.S. Matthews: *Acta Crystallogr.* **A24**, 351 (1968).
11. N. Walker and D. Stuart: *Acta Crystallogr.* **A39**, 159 (1983).
12. J. Navaza: *Acta Crystallogr.* **B50**, 157 (1994).
13. G.M. Sheldrick: *Program for crystal structure determination*. SHELX76. University of Cambridge, England (1976).
14. T.A. Jones: *J. Appl. Crystallogr.* **11**, 268 (1978).
15. Tripos Inc. SYBYL Version 5.10, Missouri, U.S.A. (1988).
16. K. Harata: *Chem. Lett.* 2057 (1986).
17. Th. Steiner and W. Saenger: *J. Am. Chem. Soc.* **114**, 10146 (1992).
18. Th. Steiner and G. Koellner: *J. Am. Chem. Soc.* **116**, 5122 (1994).
19. I. Goldberg and Z. Stein: *Acta Crystallogr.* **C40**, 666 (1994).